Geochimica et Cosmochimica Acta, Vol. 69, No. 21, pp. 5021–5032, 2005

0016-7037/05 $30.00 + .00

doi:10.1016/j.gca.2005.05.015

Diagenesis of oxyanions (V, U, Re, and Mo) in pore waters and sediments from a continental margin

JENNIFER L. MORFORD,[1,†,*] STEVEN R. EMERSON,[2] ERIN J. BRECKEL,[2] and SUK HYUN KIM[2]

[1]Woods Hole Oceanographic Institution, Marine Chemistry and Geochemistry Department, Woods Hole, MA 02543
[2]University of Washington, School of Oceanography, Seattle, WA 98195

(*Received August* 9, 2004; *accepted in revised form May* 10, 2005)

Abstract—This research tests the hypothesis that trace metals respond to the extent of reducing conditions in a predictable way. We describe pore water and sediment measurements of iron (Fe), manganese (Mn), vanadium (V), uranium (U), rhenium (Re), and molybdenum (Mo) along a transect off Washington State (USA). Sediments become less reducing away from the continent, and the stations have a range of oxygen penetration depths (depth to unmeasurable O_2 concentration) varying from a few millimeters to five centimeters. When oxygen penetrates ~1 cm or less, Fe is reduced in the pore waters but reoxidized near the sediment-water interface, preventing a flux of Fe^{2+} to overlying waters, whereas Mn oxides are reduced and Mn^{2+} diffuses to overlying waters. Both Re and U authigenically accumulate in sediments. Only at the most reducing location, where the oxygen penetrates 0.3 cm below the sediment-water interface, does the surface 30 cm of sediments become reducing enough to authigenically accumulate Mo.

Stations in close proximity to the Juan de Fuca Ridge crest are enriched in Mn and Fe from hydrothermal plume processes. Both V and Mo clearly associate with Mn cycling, whereas U may be associating with either Mn oxides and/or Fe oxyhydroxides. Rhenium is uncomplicated by adsorption to Mn oxides and/or Fe oxyhydroxides, and Re accumulation in sediments appears to be due solely to the extent of reducing conditions. Therefore, authigenic sediment Re enrichment appears to be the best indicator for intermediate reducing conditions, where oxygen penetrates less than ~1 cm below the sediment-water interface, when coupled with negligible authigenic Mo enrichment.

1. INTRODUCTION

Oceanic and atmospheric carbon cycles are strongly coupled, with the ocean reservoir of dissolved inorganic carbon being 60 times larger than that of the atmosphere (Broecker and Peng, 1987). Models that couple both ocean and atmosphere have been used to investigate why atmospheric carbon dioxide ($pCO_{2,atm}$) was reduced during the last glacial age, and thus may be useful in predicting the environmental impact of future changes in $pCO_{2,atm}$. Some of these models require a large increase in organic carbon export, through the more efficient use of nutrients, to predict the lower $pCO_{2,atm}$ observed during the last glacial age (Knox and McElroy,1984; Sarmiento and Toggweiler, 1984; Siegenthaler and Wenk, 1984). Greater organic carbon export increases the flux of carbon dioxide from the atmosphere to the ocean, thereby lowering $pCO_{2,atm}$. However, the consequence of greater organic carbon export in the ocean is the depletion of oxygen in bottom waters by organic matter oxidation (Knox and McElroy,1984; Sarmiento and Toggweiler, 1984; Siegenthaler and Wenk, 1984; Sarmiento and Orr, 1991). Widespread sustained ocean anoxia during the last glacial maximum is unrealistic, based on observations of sediment cores from that time period which indicate well mixed sediments indicative of biologic activity and oxic conditions. It is possible, however, that bottom water oxygen concentrations decreased dramatically, because there are presently no acceptable tracers of bottom water oxygen concentration. Development of reliable tracers for organic carbon flux to the sediment-water interface and bottom water oxygen concentration would provide a dramatic improvement on the understanding of redox conditions in the ocean and help constrain theories for the reduction of atmospheric pCO_2 during glacial times.

The combination of organic carbon rain rate and bottom water oxygen concentration determines the extent of reducing conditions in surface sediments. Oxygen is the primary oxidant for the degradation of organic matter; in the absence of oxygen, however, other species oxidize organic matter following a thermodynamically predicated sequence of oxidants (oxygen → manganese oxides ~ nitrate → iron oxyhydroxides → sulfate; Froelich et al., 1979). Therefore, in the absence of oxygen, pore water concentrations of Mn^{2+} and/or Fe^{2+} can be indicative of Mn oxide and Fe oxyhydroxide reduction, respectively. However, the absence of pore water Mn^{2+} and/or Fe^{2+} does not imply Mn and/or Fe reduction is not occurring, and interpretation of pore water profiles must include careful attention to both pore water and sediment species. In the absence of irrigation of sediments by macrofauna (Aller, 1990), the steady-state oxidation state of sediment pore waters is indicated by the penetration depth of O_2 below the sediment-water interface (Morford and Emerson, 1999). Perturbation of the steady-state situation by either an increase in the flux of organic matter, due to either an increase in overlying productivity or in sedimentation rate or a decrease in bottom water oxygen, would result in an increase in the reducing conditions and a shoaling of the oxygen penetration depth.

Concentrations of redox-sensitive trace metals (U, Re, V, and Mo), which are soluble under oxic conditions but precip-

* Author to whom correspondence should be addressed (jennifer.morford@fandm.edu).
† *Present address:* Franklin and Marshall College, Department of Chemistry, P.O. Box 3003 Lancaster, PA 17604–3003.

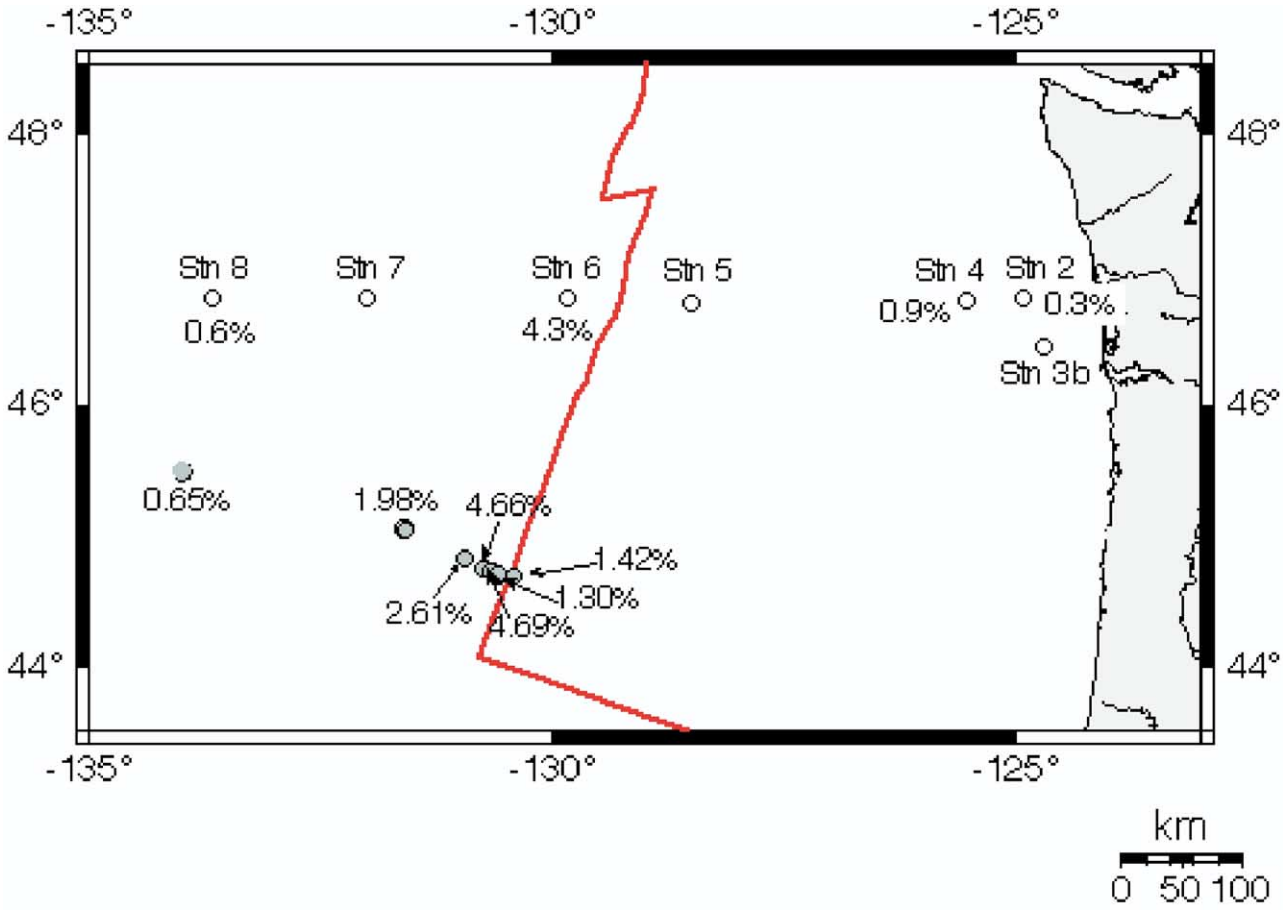

Fig. 1. Map of station locations for stations 2, 3b, 4, 5, 6, 7, and 8 (open circles). The transect extends off Washington State and continues to the west side of the Juan de Fuca Ridge crest, denoted by the line between stations 5 and 6. Surface Mn concentrations (% by weight) are included for stations 2, 4, 6, and 8. Literature data for surface Mn concentrations are also plotted to the south of the transect (shaded circles, data from Table 2 in Lavelle et al., 1992).

itate (or adsorb) under anoxic conditions, have been used to identify the redox state of sediments. There has been extensive research of these elements under oxic and anoxic conditions (e.g., Anderson et al., 1989; Barnes and Cochran, 1991, 1993; Wanty and Goldhaber, 1992; Colodner et al., 1993; Calvert and Pedersen, 1993), but more recent research has focused on continental margin settings where intermediate reducing conditions prevail (Shaw et al., 1990; Klinkhammer and Palmer, 1991; Barnes and Cochran, 1993; Crusius et al., 1996; Morford and Emerson, 1999; Nameroff et al., 2002; Zheng et al., 2002; Sundby et al., 2004). Using our present understanding of trace metal geochemical cycling in recent sediments, interpretation of changes in sediment metal concentrations deposited over time have been used to suggest changes in redox conditions (e.g., Calvert and Pedersen, 1993; François et al., 1993, 1997; Dean et al., 1994, 1997, 1999; Rosenthal et al., 1995; Crusius et al., 1996, 2000; Anderson et al., 1998; Adelson et al., 2001; Nameroff et al., 2004). However, the use of redox-sensitive metals as indicators of past environmental conditions is limited by an incomplete understanding of their geochemical cycling in present-day conditions, and the potential for diagenetic changes that obscure the sedimentary signal are not well understood (e.g. for U: Mangini et al., 2001). The primary goal of this paper is to characterize metal behavior in recent sediments across a continental margin transect, using both pore water and sediment metal profiles, and to determine the optimal trace element(s) for identifying intermediate reducing conditions.

2. SITE DESCRIPTION

Cruise TTN-131 (2001) followed and extended a transect previously described in Hedges et al. (1999) and Devol and Hartnett (2001). The transect was primarily along 47°N from the continental shelf off Washington State (U.S.A.) to the west side of the Juan de Fuca Ridge (~133°W) (Fig. 1; Stump and Emerson, 2001). Carbon rain rates have been shown to be higher closer to the continent, approximately 180 μmol cm^{-2} yr^{-1} at 440 m water depth, and decrease dramatically with increasing water depths (approximately 70 μmol cm^{-2} yr^{-1} by 620 m water depth; Devol and Hartnett, 2001). The water column–dissolved oxygen distribution shows an oxygen minimum extending from approximately 700 to 1100 m water depth (Hartnett and Devol, 2003; Devol and Hartnett, 2001); however, oxygen concentrations are always greater than 20 μM and denitrification in the water column is not an important process (Hartnett et al., 1998). Sampling across the oxygen

Table 1. Station information for cruise TTN-131 (July 23-August 3, 2001) (Stump and Emerson, 2001). The transect extends from ~47° N to ~133° W and encompasses a range of water depths. Oxygen penetration depths were determined by oxygen microelectrode (A. Devol, pers. comm.). Sedimentation rates are based on cores recovered previously from relatively close stations (Hedges et al., 1999; Lambourn et al., 1996).

Station	Lat (°N), Long (°W)	Water depth (m)	$[O_2]_{BW}$ (μM)	Oxygen penetration depth (cm)	Sedimentation Rate (cm kyr^{-1})
2MC39	46°47.83,124°54.40	434	40	0.3	15
3bMC10	46°25.56,124°41.50	1136	14	0.4	10
4MC33	46°46.48,125°31.55	1961	55	0.5	12
5MC30	46°44.98,128°30.01	2759	81	2.5	2.5
6MC17	46°46.99,129°49.99	2807	81	1.5	2
7MC26	46°47.00,132°00.00	3232	115	1.4	2
8MC22	46°47.00,133°39.99	3866	124	5.0	2

minimum zone and along a gradient of carbon export resulted in a range of sediment oxygen penetration depths (Table 1, Fig. 2). Stations 2, 3b, and 4 have oxygen penetration depths that are less than 1 cm, whereas stations 5, 6, 7, and 8 have oxygen penetration depths that extend from 1.4 cm to 5 cm.

3. METHODS

3.1. Sampling Method

Sediment cores (30–60 cm in length) with clearly defined sediment-water interfaces and overlying waters that were clear of resuspended sediment upon recovery were collected using a multicorer. Cores were immediately capped with plastic-wrapped rubber stoppers and moved to a 4°C room. All core processing occurred at 4°C in a refrigerated van while at sea. The overlying waters were sampled and the cores were then sectioned in a nitrogen-filled glove bag. The resolution for the first 12 samples was determined by filling scintillation and centrifuge vials. By knowing the volume of the vials and the diameter of the core, the depth sampled was calculated. The first six samples were from intervals of ~0.35 cm, and samples 7–12 were from depth intervals of ~0.6 cm. This sampling method required sampling across the entire surface, including sediment against the core liner; however, sharp metal profiles in the top 12 samples suggest minimal profile smearing (see later section). Sediment sampling continued at 1 cm or 2 cm intervals to the bottom of the core.

Sediments were centrifuged and pore waters were filtered in a nitrogen-filled glove bag, using nitrogen-flushed syringes and 0.45-μm filters, and transferred to 4-mL acid-cleaned HDPE bottles, which were spiked with 75 μL concentrated double-distilled nitric acid. Prior to the cruise, syringes and filters were cleaned with 2 M HCl, rinsed with 18 MΩ MilliQ water, and dried in a laminar flow hood. Sample storage 4-mL HDPE bottles were filled with 2 M HCl for four days at 60°C, rinsed with 18 MΩ MilliQ water, and dried in a laminar flow hood.

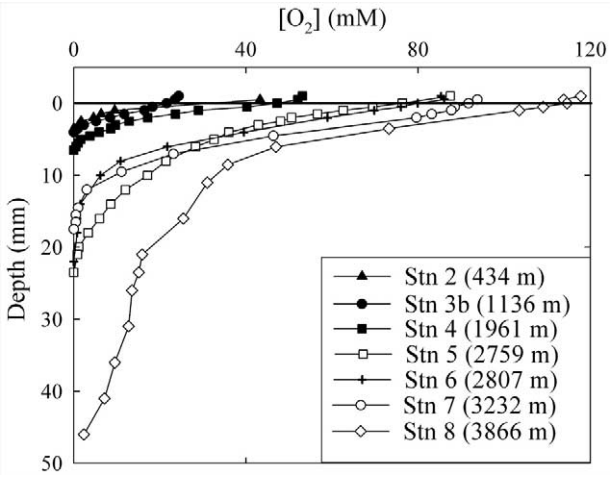

Fig. 2. Oxygen microelectrode profiles for stations 2, 3b, 4, 5, 6, 7, and 8 (data from A. Devol, University of Washington).

3.2. Analysis Methods—Pore Waters and Sediments

Pore waters were diluted 20-fold with approximately 0.8 M HNO_3 and spiked with an internal standard solution (Sc, Y, In, Cs, Lu) following the method of Rodushkin and Ruth (1997). This relatively simple method with minimal sample preparation allows for the simultaneous quantification of Fe, Mn, V, U, Mo, and Re, without preconcentration techniques or other preanalysis sample preparations. The samples were run on a Finnigan Element high-resolution inductively coupled plasma-mass spectrometer (HR-ICPMS) at the Woods Hole Oceanographic Institution, in both low (V, U, Mo, Re) and medium (Mn, Fe) resolution settings. Solutions composed of a combination of single-element standards containing Fe, Mn, V, U, Mo, Re and internal standards (Sc, Y, In, Cs, Lu) were run with samples to assess and correct for instrument mass bias. Replicate measurements of CASS-4 (Nearshore Seawater Reference Material for Trace Metals, National Research Council, Canada) and overlying water samples were used to determine method accuracy and precision.

Dried sediments were completely dissolved using a modification of the method of Murray and Leinen (1993) as described by Morford and Emerson (1999). Rhenium was manually preconcentrated prior to analysis using AG1 X8 100–200 mesh chloride-form resin (modified from Colodner, 1991). All sediment samples were analyzed using a Perkin Elmer Elan 5000 ICPMS at the University of Washington in peak jumping mode, as described in Morford and Emerson (1999), except for Fe and Al, which were measured using a flame atomic absorption spectrometer. Duplicate digestions and analyses of sediment samples were used to assess precision. Daily analyses of PACS-1 (Marine Sediment Reference Materials for Trace Metals and Other Constituents, National Research Council, Canada) and correlations with certified

Table 2. Replicate analyses of CASS-4 Nearshore Seawater Reference Material (n = 17– 20). The measured values are reported as the average concentration (nM) ± standard deviation (percent relative standard deviation, %RSD), whereas the known CASS-4 concentration is reported with its standard deviation at the 95% confidence limit.

[Element] (nM)	Measured CASS-4	Known CASS-4
Mn	52.3 ± 6.8 (13%)	50.6 ± 3.5
V	29.3 ± 3.8 (13%)	23.2 ± 3.1
U	10.6 ± 0.8 (8%)	12.6*
Mo	94.8 ± 8.9 (9%)	91.5 ± 9.0
Re ($\times 10^{-3}$)	35 ± 5 (15%)	NV

* Note: The known U concentration in CASS-4 is only for information and is not certified.
NV indicates that neither a certified nor a recommended value is available.

Table 3. Replicate analyses of overlying water (OVW) from station 2 (n = 9), triplicate analyses of station 6, and duplicate analyses from stations 1, 4, 5, 7, 8. Average overlying water concentrations are compared with known dissolved ocean concentrations. Duplicate analyses of a sample from station 3b taken from 0.9 cm below the sediment-water interface are also included. The measured values are reported as the average concentration (%RSD). Duplicate samples were typically run the same day; overlying water from station 2 was analyzed with every ICP-MS run.

	Fe (μM)	Mn (μM)	V (nM)	U (nM)	Mo (nM)	Re (pM)
Stn 2 OVW	<DL	<DL	43.6 (8.9%)	12.2 (5.4%)	106 (6.8%)	39 (17%)
Stn 6 OVW	<DL	<DL	65.2 (8.7%)	12.8 (0.7%)	113 (2.7%)	38 (12%)
Stn 1 OVW	<DL	<DL	54.4 (12%)	12.3 (0.9%)	114 (0.5%)	36 (10%)
Stn 4 OVW	<DL	<DL	49.0 (4.4%)	11.4 (0.4%)	92.3 (8.2%)	36 (8.4%)
Stn 5 OVW	<DL	<DL	34.4 (1.5%)	10.6 (2.5%)	89.5 (1.5%)	50 (22%)
Stn 7 OVW	<DL	<DL	58.9 (7.3%)	12.5 (2.1%)	112 (5.0%)	35 (11%)
Stn 8 OVW	<DL	<DL	49.7 (cont.)	12.6 (1.3%)	112 (0.5%)	55 (cont.)
Average OVW	na	na	48.2 (20%)	12.1 (8.0%)	106 (8.6%)	39 (19%)
Dissolved ocean conc.	na	na	35–45[a]	14[b]	105[c]	39–45[d]
Stn 3B 0.9 cm	0.9 (2.7%)	0.7 (0.8%)	40.8 (3.2%)	10.5 (0.6%)	120 (5.0%)	54 (13%)

<DL denotes below detection limit, na denotes not applicable, cont. denotes that one of the replicates was contaminated. a. Collier (1984); Jeandel et al. (1987); b. Ku et al. (1977); c. Collier (1985); d. Colodner (1991); Anbar et al. (1992).

concentrations were used to assess accuracy of measured sediment sample concentrations.

3.3. Method Results—Accuracy and Precision

Reproducibility and accuracy of pore water analyses were calculated using replicate measurements of CASS-4 and overlying water samples. The measurement reproducibility of CASS-4 and overlying waters is ≤20% for Re, Mn, and V and <10% for U and Mo (Tables 2 and 3). Duplicate samples from station 3b, taken from 0.9 cm below the sediment-water interface, were measured to determine the precision for Fe, which was <5% (Table 3). Manganese and Mo are within the 95% confidence interval of the known concentration for CASS-4, whereas there is no known Re concentration reported for CASS-4. The average overlying water Mo and Re concentrations are consistent with their known oceanic concentrations within the measurement error. The average measured V concentration is ~26% higher than the certified CASS-4 concentration, and higher overlying water V concentrations were measured relative to the expected range in literature seawater concentrations (Table 3). The U concentration is not certified for the CASS-4 standard; however, measured U concentrations are 16% lower than the recommended concentration (Table 2) and overlying water U concentrations are 13% lower than the known seawater concentration (Table 3). Therefore, the results from Tables 2 and 3 suggest that V analyses are somewhat high (0%–25%) and U analyses are 10%–20% low. We believe this is due to inaccuracy in our relatively simple analytical method involving only a 20-fold sample dilution and internal standards. A more rigorous method, in which the salts are removed from the sample prior to analysis and/or isotope dilution is used for quantification, would have resulted in better accuracy for V and U. However, because our interpretations focus on changes between bottom water and pore water concentrations, the inaccuracy of the method will not affect the following discussion.

The reproducibility of the sediment analyses (Table 4) was determined by duplicate analyses of samples. Reproducibility of measurements are ≤5% for Ti, Fe, and V and ≤8% for Mo, Al, Mn, U, and Re (for Re samples above 1 ppb, Table 4). Accuracies were determined by measuring sediment reference standards when available. Accuracies were better than 6% for all metals (for details, see Breckel et al., 2004). The dramatically improved accuracy and precision reported for sediment Re concentrations relative to pore water Re measurements are most likely due to the preconcentration and isotope dilution method used for the sediment samples.

4. RESULTS AND DISCUSSION

4.1. Titanium Sediment Results

Stations 2, 4, 6, and 8 have relatively constant Ti/Al sediment ratios similar to the Ti/Al ratio found in shale (Fig. 3; Turekian and Wedepohl, 1961). The Ti/Al ratio in sediments may be a tracer for grain size and detrital source. Higher Ti/Al ratios may indicate larger grain sizes (Spears and Kanaris-Sotiriou, 1976) or a change in the detrital source from shales to more basaltic-type rocks, which have higher Ti concentrations (Turekian and Wedepohl, 1961). Therefore, measured Ti/Al ratios suggest the absence of coarse-grained material and the appropriateness of shale as an estimate for detrital concentrations.

4.2. Iron and Manganese

An examination of both pore water and sediment profiles can yield insight into the controls on Fe and Mn fluxes from sediments to overlying waters. Pore water Fe concentrations are elevated below 1 cm at stations 2 and 3b and below about 5 cm

Table 4. Average concentrations (%RSD) are presented for duplicate analyses of sediment samples.

	Depth (cm)	[Al] (%)	[Ti] (%)	[Fe] (%)	[Mn] (ppm)	[V] (ppm)	[U] (ppm)	[Mo] (ppm)	[Re] (ppb)
Stn 2	0.3	5.40 (5.6%)	0.35 (1.2%)	11.1 (2.4%)	323 (0.3%)	104 (0.9%)	1.31 (1.5%)	0.63 (2.2%)	3.47 (5.7%)
	7.7	6.75 (0.0%)	0.42 (0.2%)	7.63 (5.0%)	383 (0.6%)	117 (2.9%)	2.52 (2.5%)	1.32 (3.6%)	8.33 (3.69%)
Stn 4	7.2	8.26 (4.3%)	0.49 (3.9%)	4.83 (4.6%)	427 (5.2%)	133 (3.5%)	2.58 (4.6%)	0.72 (4.8%)	5.13 (4.0%)
	31.7	7.39 (0.23%)	0.50 (3.1%)	4.38 (0.08%)	405 (7.1%)	124 (0.6%)	4.17 (3.2%)	1.12 (7.6%)	13.57 (5.4%)
Stn 6	9	6.02 (0.8%)	0.34 (0.09%)	5.24 (3.1%)	29350 (0.5%)	165 (1.3%)	1.74 (0.4%)	7.57 (1.2%)	0.26 (33%)
	27	6.98 (6.7%)	0.41 (4.6%)	5.63 (3.2%)	5370 (0.3%)	147 (3.3%)	1.34 (5.6%)	1.55 (0.6%)	1.16 (8.0%)
Stn 8	2.5	8.50 (0.4%)	0.47 (1.5%)	5.04 (3.5%)	6330 (1.8%)	137 (0.9%)	1.64 (5.1%)	5.29 (0.9%)	0.07 (11%)
	21	8.44 (5.7%)	0.48 (0.6%)	4.88 (0.8%)	5140 (0.3%)	132 (0.4%)	1.70 (1.4%)	2.97 (0.6%)	0.08 (10%)

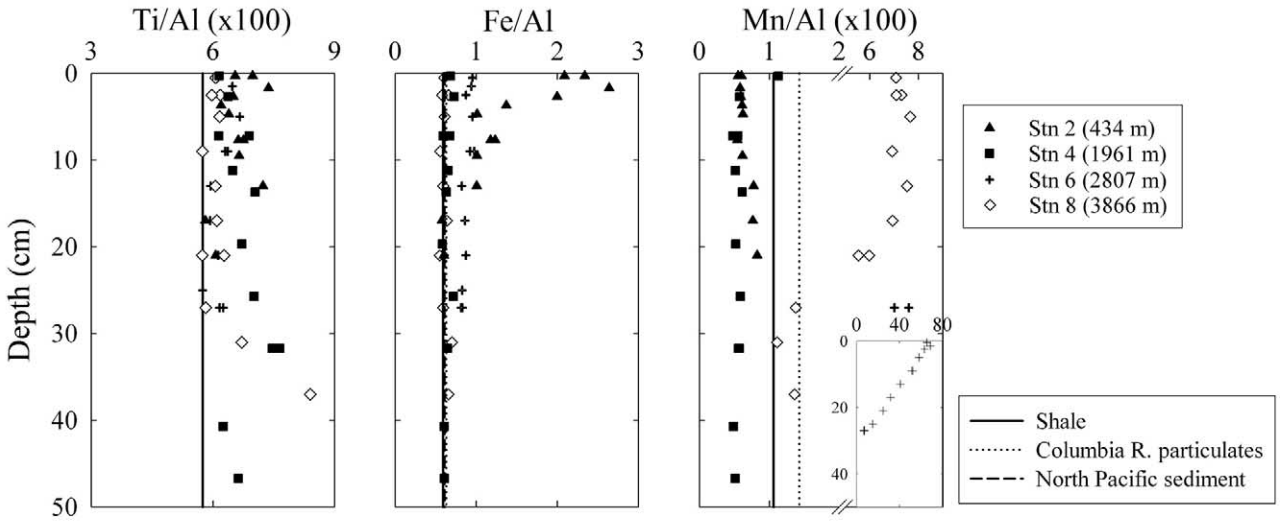

Fig. 3. Metal/aluminum ratios for Ti, Fe, and Mn in sediment cores plotted against depth (cm) for stations 2, 4, 6, and 8. The vertical lines denote various metal/Al detrital estimates.

at station 4 (Fig. 4). Surface sediment authigenic Fe enrichment at station 2 is consistent with remobilization and precipitation at the sediment-water interface (Fig. 3). The pore water gradient at station 4 is sufficiently less steep to prevent detectable enrichment in the surface sediments. Therefore, Fe does not appear to diffuse to overlying waters, implying that Fe cycling is restricted to sediments and pore waters and does not extend to overlying waters, which is consistent with the results of Thamdrup et al. (1994) for coastal systems.

Pore water Mn^{2+} is below 8 μM in all pore waters from stations 2, 3b, and 4, where oxygen penetrates less than 1 cm. The pore water Mn^{2+} profiles suggest that Mn oxide reduction is occurring very close to the sediment-water interface where Mn^{2+} can diffuse to the overlying waters (Fig. 4). The sediment profiles from stations 2 and 4 are consistent with this interpretation, suggesting Mn depletion relative to detrital estimates (Fig. 3). Whereas Fe cycling appears to be restricted to sediments and pore waters, Mn cycling extends to overlying waters. The reason for the difference is the relative oxidation rate kinetics of these metals, which results in rapid Fe^{2+} oxidation (Sung and Morgan, 1980) preventing Fe depletion in surface sediments (Fig. 3). Manganese oxidation rates, however, are typically on the time scale of days to weeks in the presence of particulate surfaces (Davies and Morgan, 1989) or

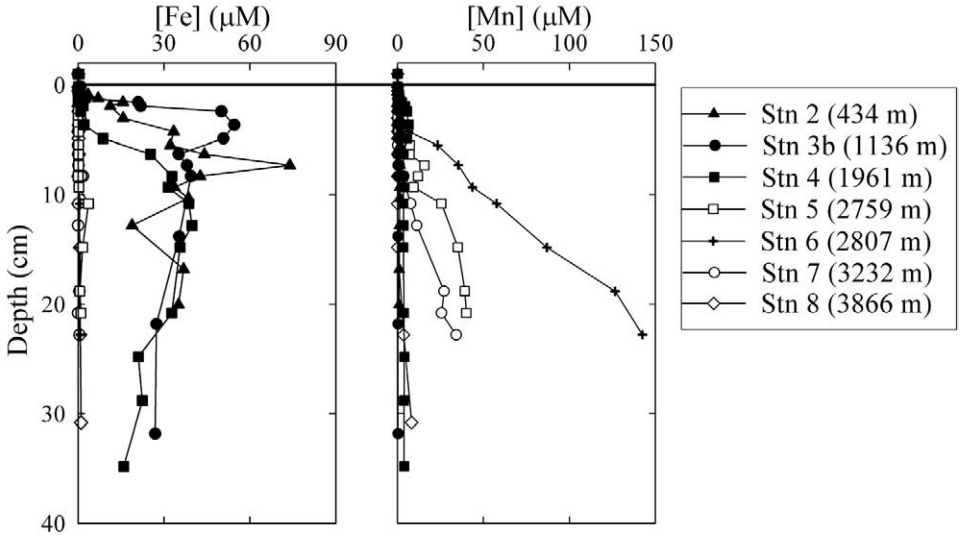

Fig. 4. Pore water Fe^{2+} and Mn^{2+} concentrations versus depth for all stations. Note that stations 2, 3b, and 4 have oxygen penetration depths of <1 cm whereas stations 5, 6, 7, and 8 have oxygen penetration depths of >1 cm. The horizontal lines denote the sediment-water interface.

when microbially mediated (Tebo et al., 1984). Only where Mn oxide reduction is occurring deep enough in pore waters to build up pore water Mn^{2+} does oxidation in surface sediments limit the Mn flux to overlying waters. High concentrations of pore water Mn^{2+} are measured below ~5–10 cm depth in cores from stations 5, 6, and 7 (Fig. 4). Iron oxyhydroxide reduction is probably occurring at these stations, but oxygen, nitrate, or Mn oxides (Myers and Nealson, 1988) may be used to oxidize Fe^{2+}, thereby removing Fe^{2+} from pore waters and resulting in measurable Mn^{2+} in pore waters. Station 6, which is close to the Juan de Fuca Ridge crest, is probably influenced by hydrothermal activity, resulting in high Mn^{2+} concentrations (Fig. 4) and both Mn and Fe sediment enrichment (Fig. 3, see later discussion). Only at station 8 are both Mn^{2+} and Fe^{2+} absent from upper pore waters; however, hydrothermally influenced sediment Mn enrichment is apparent throughout the top 28 cm of this core (Fig. 3).

4.3. Uranium and Rhenium

Pore water U and Re profiles can provide information on the geochemical cycling of these elements and, coupled with their respective sediment profiles, can provide estimates for authigenic U and Re fluxes to sediments. Pore water data suggests U removal from the dissolved form in pore waters at stations 3b and 4 to a final concentration of 2–5 nM by 5–8 cm (Fig. 5). Although the pore water data from station 2 is somewhat scattered, the pore water U concentration at the bottom of the core is also depleted to ~5–6 nM (Fig. 5). Sediment U profiles indicate authigenic U enrichment below 5 cm at stations 2 and 4 relative to detrital estimates appropriate for this location, in agreement with pore water profiles (Fig. 6). Uranium is also enriched in the top 10 cm of station 6, although there is no indication of uptake from pore waters. This location is heavily influenced by hydrothermal sediments (see later discussion), which may provide a mechanism for U enrichment (Mills et al., 1993). The change in U pore water gradients from stations 3b and 4 at approximately 5 cm and 8 cm, respectively, are coincident with the broad maxima in pore water Fe^{2+}, suggesting similar depths of reduction (Figs. 4 and 5). The extremely low pore water U concentration at ~7.3 cm at station 2 coincides with the peak in pore water Fe^{2+}, perhaps suggesting a local zone of intense Fe and U reduction. The similarity in depths for Fe and U reduction is consistent with previous pore water and sediment profiles (Cochran et al., 1986; Klinkhammer and Palmer, 1991; Crusius et al., 1996; Zheng et al., 2002). Microbial reduction of U(VI) has been shown to be associated with Fe(III)-reducing bacteria (Lovley et al., 1991); therefore, it is not unexpected that U reduction and subsequent removal from pore water would occur at similar depths as Fe reduction. The nonzero U concentrations deeper than 10 cm at stations 3b and 4 (2–4 nM) are similar to deep pore water U concentrations measured in profiles from the California margin (~4 nM) and the Mid-Atlantic Bight (~2 nM) (Zheng et al., 2002). This residual pore water U may be less than the minimum concentration necessary for microbial reduction.

The pore water Re data are extremely scattered in the top 8 cm for the majority of stations (Fig. 5), but below 8–13 cm the data are consistent and indicate Re removal from solution at stations 2, 3b, and 4 to a relatively constant concentration of

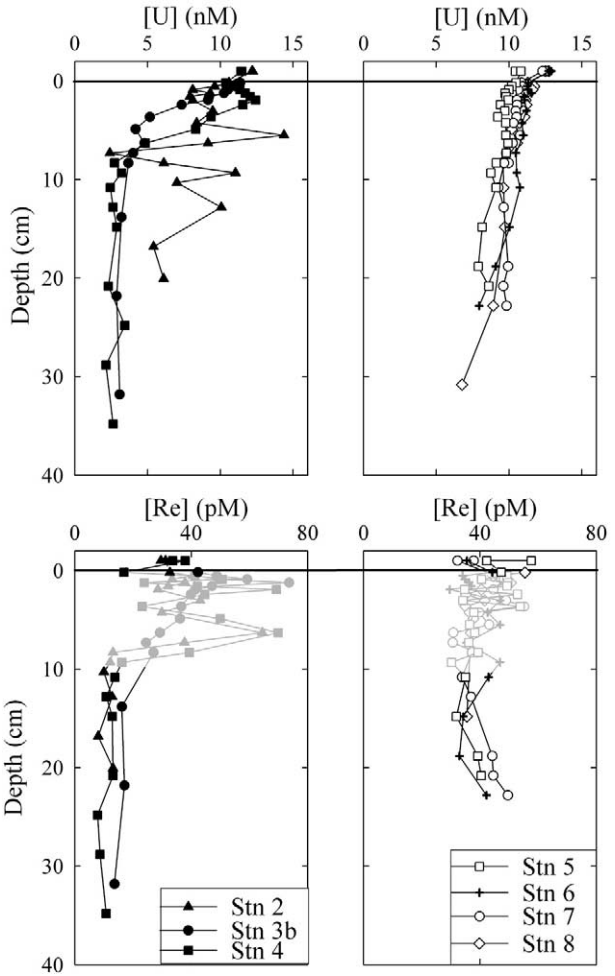

Fig. 5. Pore water U and Re concentrations versus depth for all stations. Gray symbols designate Re samples that were scattered owing to either analytical problems during analysis or oxidation artifacts during processing; see text for full explanation. See Figure 4 caption for comments.

8–17 pM and no removal from pore waters from stations 5, 6, 7, and 8 (Fig. 5). These conclusions from the pore water profiles are consistent with the Re sediment profiles that show authigenic Re enrichment at stations 2 and 4 and detrital concentrations at stations 6 and 8. The reason for the scatter of the pore water Re data in the surficial sediments is not known. The lack of sample preconcentration prior to pore water analysis resulted in HR-ICPMS sample count rates of ~100–200 counts per second relative to a blank of 5–20 cps, which could contribute to the observed signal noise and would suggest that a simple 20-fold sample dilution is not suitable for Re analysis. However, the lack of scatter for Re concentrations in samples below 10 cm suggests that this may not be the sole reason. The scatter in the top 10 cm of the Re data could also be due to oxidation artifacts that occurred during core processing. Deeper pore waters are less susceptible to oxidation because they are more reducing and tiny amounts of oxygen that reach these pore waters during processing may be consumed by oxidation of more reducing elements, such as sulfide or iron, resulting in effective redox "buffering." However, shallower pore waters

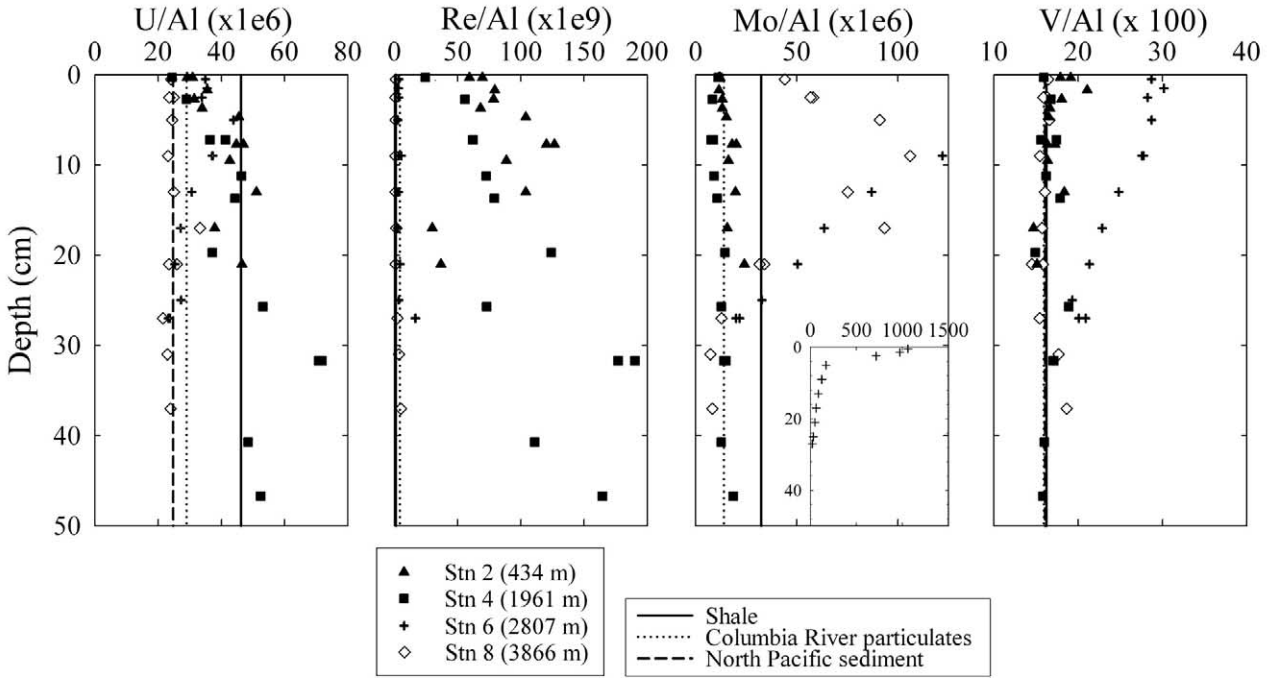

Fig. 6. Metal/aluminum ratios for U, Re, Mo, and V measured in sediment cores plotted against depth (cm) for stations 2, 4, 6, and 8. The vertical lines denote various metal/Al detrital estimates (North Pacific oxic sediments: Kyte et al., 1993; Columbia River particulates: Morford and Emerson, 1999).

may be more susceptible to oxygen introduced during core processing because this region of the sediments is relatively poorly buffered with respect to redox processes, which might result in easier oxidation of reduced sedimentary Re and remobilization to pore waters.

The scatter in pore water Re data makes it difficult to correlate with depths of Fe or U reduction. However, the pore water profiles seem to suggest a very similar depth of reduction for Re and U, which is consistent with the results of Crusius et al. (1996). Rhenium profiles from stations 2, 3b, and 4 decreased to 8–17 pM, similar to pore water Re profiles from the North Pacific that showed decreasing Re concentrations from 44 pM to ~10 pM at 17 cm (Colodner et al., 1993). Colodner et al. (1993) also presented relatively constant Mo pore water concentrations in these North Pacific cores, suggesting that Re removal occurs under less-reducing conditions relative to conditions necessary for Mo removal. This order of removal is consistent with results from stations 3b and 4 and previous research (Crusius et al., 1996).

4.4. Molybdenum and Vanadium

The combination of pore water and sediment profiles can also yield information on complexation and sedimentary controls on cycling, in addition to controls on authigenesis. Elevated pore water Mo measured in samples close to the sediment-water interface at all of the stations relative to overlying water concentrations may be due to an artifact of centrifuging, or possibly complexation with DOC in pore water (Fig. 7; Emerson and Huested, 1991). Only station 2 appears to be reducing enough to remove Mo from pore waters, with Mo concentrations decreasing from 101 nM in overlying waters to 86 nM below 10 cm (Fig. 7). The sediment profile for Mo at station 2 also shows slight authigenic enrichment below 5 cm (Fig. 6). However, it does not appear that any of the other stations are reducing enough to remove Mo from pore waters via reduction. Increasing pore water Mo concentrations with depth are coincident with increasing pore water Mn^{2+} at station 6 and suggests Mo recycling with Mn. The decrease in pore water Mo at station 7 from approximately 6–8 cm is likely due to adsorption to Mn oxides that are inferred to occur at this depth based on the pore water Mn^{2+} concentrations that approach zero at ~7 cm (Figs. 4 and 7), although we do not have sediment data for station 7 to substantiate this hypothesis. Authigenic Mo enrichment is obvious in sediments from stations 6 and 8, although this is more likely due to adsorption to Mn oxides rather than reduction (Figs. 3 and 6).

Surface pore waters from stations 4, 5, 6, 7, and 8 are enriched in V up to 350 nM, probably because of complexation with dissolved organic carbon (Fig. 7; Brumsack and Gieskes, 1983; Emerson and Huested, 1991). Pore water concentrations come to a constant concentration of 27–38 nM below 5 cm at stations 2, 3b, and 4, which is somewhat less than the V concentration in the overlying waters (40–60 nM) (Fig. 7), suggesting some V removal from pore waters. Authigenic sediment V enrichment from station 2 is apparent in the top 5 cm but not deeper, and there appears to be little enrichment at station 4 (Fig. 6). In general, both pore water and sediment concentrations of V are strongly associated with Mn cycling. Data from station 6 suggest V association with Mn cycling through both elevated pore water V concentrations below 6 cm and elevated Mn^{2+} pore water concentrations (Figs. 4 and 7),

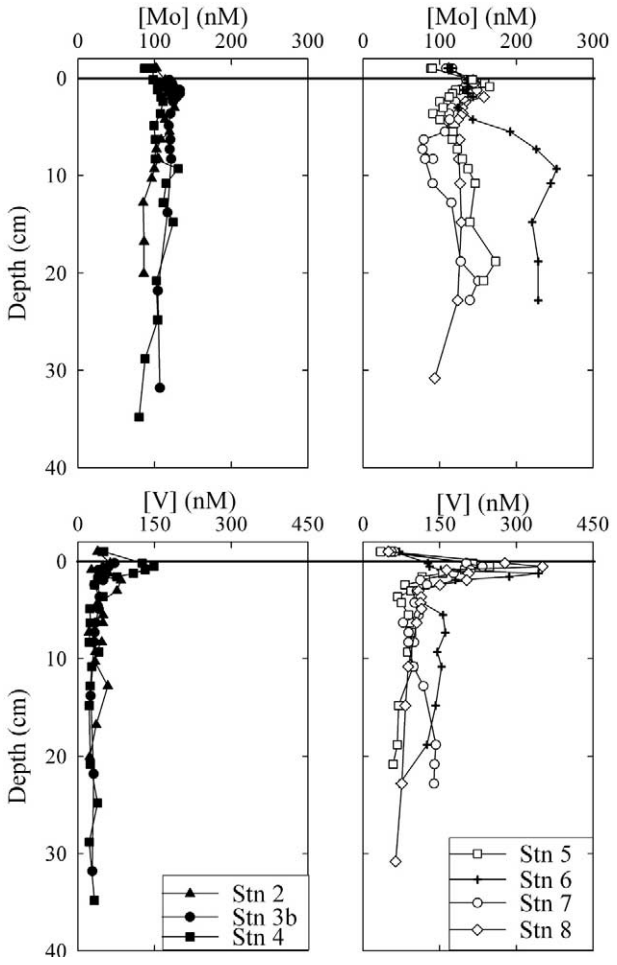

Fig. 7. Pore water Mo and V concentrations versus depth for all stations. See Figure 4 caption for comments.

suggesting that both Mn^{2+} and V are released during Mn oxide reduction. Station 6 sediment V concentrations are also elevated concurrent with elevated Mn sediment concentrations (Figs. 3 and 6), suggesting V adsorption to Mn oxides.

4.5. Hydrothermal Influence at Stations 6 and 8

Both sediment and pore water profiles at stations 6 and 8 suggest tht reducing conditions are not solely responsible for metal cycling. There are large authigenic sediment Mn enrichments measured at both stations, which decrease below 20 cm to detrital concentrations in the case of station 8. Pore water Mn concentrations are also high at depth for station 6 (150 μM). Calculations of the upward diffusion of pore water Mn^{2+}, however, suggest that the pore water flux cannot adequately supply a steady-state accumulation of surface sediment Mn enrichment (Table 5). The upward flux of Mn^{2+} (F_{pw}) is approximately 50% and 29% of the sediment accumulation rate of Mn (F_{sed}) for stations 6 and 8, respectively. Therefore, the flux of Mn into sediments is greater than the pore water flux, which suggests nonsteady-state accumulation and additional Mn input from above.

Sediment Mn enrichment above detrital concentrations at stations 6 and 8 is due to hydrothermal input from the nearby Juan de Fuca Ridge crest. The distribution of surface sediment Mn concentrations along a transect south of the data presented here suggests a stronger hydrothermal input extending to the west, with higher surface Mn sediment concentrations closer to the ridge crest and smaller Mn enrichments approximately 300 km from the ridge crest (Fig. 1; Lavelle et al., 1992). The Mn distribution presented here is similar to the data presented by Lavelle et al. (1992) and is consistent with elevated Mn occurring off axis and decreasing but still elevated several hundred meters away. A hydrothermal input would also explain the Fe sediment profile at station 6, which is elevated throughout the profile (Fig. 3). This Fe profile suggests a constantly enriched Fe concentration, consistent with Fe enrichment due to hydrothermal precipitates (Dymond, 1981; Heath and Dymond, 1981; Klinkhammer and Hudson, 1986; Schaller et al., 2000).

The decreasing Mn sediment enrichment with increasing depth at station 6, however, cannot be explained by steady-state hydrothermal input. It is possible that the hydrothermal input has not been constant, with a greater hydrothermal input during more recent times. However, changing hydrothermal input would not be consistent with the relatively constant Fe/Al ratio measured in sediments from station 6. It is possible that the profile results from a change in reducing conditions over time. For example, if the present-day conditions are more reducing than those at approximately 10 kyr B.P., when the sediment at 20 cm was deposited, then the increase in reducing conditions

Table 5. Calculation of pore water Mn^{2+} fluxes and Mn sediment accumulation rates at stations 6 and 8. The upward flux of Mn^{2+} is calculated as $F_{pw} = D_{sed} * \varphi * \frac{d[Mn^{2+}]}{dz}$, where F_{pw} is the flux of Mn^{2+} through pore waters, D_{sed} is 1.9×10^{-6} cm^2 s^{-1} (Bender, 1971), porosity (ϕ) is assumed to be 0.8 cm^3_{water} cm^{-3}_{bulk}, and the change in Mn^{2+} concentration ($d[Mn^{2+}]$) is from the bottom of the core to the depth at which $[Mn^{2+}] = 0$. The sediment Mn accumulation rate is calculated as $F_{sed} = s\rho(1 - \phi)\,[Mn]_{authr}$. The sedimentation rate (s) is based on relatively close stations (Table 1), and the sediment density (ρ) is assumed to be 2.5 g_{sed} cm^{-3}_{sed}. The authigenic sediment Mn concentrations reflect the Mn added after sediment deposition and are calculated as the difference between the measured and detrital (background) concentrations. The authigenic concentrations are calculated as $[Mn]_{auth} = [Mn]_{total} - \left([Al]_{total} x \frac{[Mn]_{detrital}}{[Al]_{detrital}}\right)$, where the detrital Mn/Al ratio (Columbia River particulates, Morford and Emerson, 1999) is multiplied by the Al concentration in surface sediments, and the corrected detrital Mn concentration is then subtracted from the total Mn concentration ($[Mn]_{total}$) measured in surface sediments.

	Station 6	Station 8
Depth at which $[Mn^{2+}] = 0$ (cm)	3	15
$[Mn^{2+}]$ at 23 cm (stn 6) or 30 cm (stn 8) (μM)	150	4
Upward flux of Mn^{2+} (F_{pw}, g cm^{-2} yr^{-1})	2.1×10^{-5}	0.14×10^{-5}
Sediment $[Mn]_{auth}$ (ppm)	42,200	4,810
Sedimentation rate (cm kyr^{-1})	2.0	2.0
Sediment Mn accumulation rate (F_{sed}, g cm^{-2} yr^{-1})	4.2×10^{-5}	0.48×10^{-5}
Imbalance between pore water flux and sediment accumulation rate ($F_{pw}/F_{sed}\times100$)	50%	29%
Mn accumulation due to diagenesis ($F_{sed} - F_{pw}$, g cm^{-2} yr^{-1})	2.1×10^{-5}	0.34×10^{-5}

Table 6. Data compilation for Re accumulation rate calculations.

Location	Station	$O_{2pendep}$ (cm)◆	Depth range averaged (cm)	[Re] (ppb)+	Sed Rate (cm kyr^{-1})*	Re accumulation rate (ng cm^{-2} kyr^{-1})
NW US Margin (This work)	2	0.3	8–21 cm	5.6	15	210
	4	0.5	7–47 cm	8.8	12	260
	6	1.5	9–27 cm	0.4	2	1.9
	8	5	9–37 cm	0.2	2	0.9
NW US Margin (Morford and Emerson, 1999)	WEC204	0.3	7–15 cm	5.3	15	200
	WEC213	0.6	13–28 cm	14.5	15	540
	WEC206	0.9	13–38 cm	5.9	12	180
	WEC203B	0.9	13–42 cm	9.1	12	270
African Margin (Morford and Emerson, 1999)	1BC	0.9	7–16 cm	12.5	14	420
	3BC	3	7–16 cm	7.7	3	54
	2BC	>3	6–16 cm	0.2	2	1
CA Borderlands+	Patton Escarpment	2	11–28 cm	0.7	25	43
	San Clemente	0.4	11–23 cm	8.8	25	550
	San Nicolas	0.1	13.5–25.5 cm	22.7	25	1400
	Santa Cruz	0.1	7.5–16.5 cm	12.3	25	770
Laurentian Trough (Sundby et al., 2004)	1	0.7 (±0.5)				354
	2	0.4 (±0.7)				465
	3	0.4 (±0.2)				223
	4	0.8 (±0.3)				261

◆ Oxygen penetration depths for Patton Escarpment and San Clemente are from Shaw et al., 1990. The oxygen penetration depths for San Nicolas and Santa Cruz basins are based on Mn pore water and sediment profiles (Shaw et al., 1990), which suggest extremely shallow oxygen penetration below the sediment- water interface. Oxygen penetration depths for the Laurentian Trough stations are average values for nearby cores from Silverberg et al., 2000.

+ Rhenium concentrations for the CA Borderlands are from D. Colodner, as reported in Zheng, 1999.

* All sedimentation rates for the NW US Margin are from Hedges et al. (1999) (Table 1). Sedimentation rates for the NW African Margin are from Morford and Emerson (1999) (station 2BC is assumed, based on available data). Sedimentation rates for CA Borderlands are from Emerson (1985) and references therein.

may be remobilizing a previous Mn sediment peak and concentrating it in the surface oxic sediments. Therefore, high surface sediment Mn concentrations could be due to diagenetic Mn remobilization at depth, upward migration of Mn^{2+}, oxidation, and additional scavenging of dissolved hydrothermal Mn^{2+} on oxide surfaces. This would augment the Mn enrichment at the surface and would explain the continuously decreasing Mn concentration with increasing depth. The hypothesis of less-reducing conditions ~10 kyr B.P. is difficult to verify from other sediment cores along the northeast Pacific, because the sedimentation rate has not been precisely determined at station 6. However, organic carbon results from off Oregon State suggest reduced primary productivity from 11.6 to 13.6 kyr B.P., possibly coincident with the Younger Dryas, a result of reduced coastal upwelling in this area (Kienast et al., 2002, and references therein).

The presence of both Mn and Fe enrichment at stations 6 and 8 also highlights the association of trace metals with oxide surfaces. The sediment V profile for station 6 has a similar profile to Mn, suggesting adsorption to Mn oxides, which is consistent with previous research (Calvert and Piper, 1984; Wehrli and Stumm, 1989). Decreasing sediment V concentrations with increasing depth at this location may also suggest V release from Mn oxides during Mn oxide reduction. The Mo enrichment at station 6 is more concentrated at the surface, perhaps suggesting a stronger association with freshly precipitating Mn oxides. Molybdenum is also enriched in sediments from station 8, with a profile similar to Mn. Uranium sediment enrichment is only obvious at station 6 and could be due to association with either Mn oxides or Fe oxyhydroxides, which is consistent with previous research (Barnes and Cochran, 1991). An additional hydrothermal U input is also possible, because U is strongly enriched in hydrothermal sulfide deposits (Mills et al., 1993). Rhenium is at detrital concentrations for both stations, concurring with results from Colodner et al. (1993) and Crusius et al. (1993), who found no relation with Mn or Fe cycling. In addition, Re has not been found to be associated with hydrothermal processes (Ravizza et al., 1996; Schaller et al., 2000).

4.6. Rhenium as a Model Tracer for Intermediate Reducing Conditions

A compilation of literature shows large Re accumulation rates (>100 ng cm^{-2} kyr^{-1}; Table 6 and Fig. 8) when oxygen penetration depths are less than ~1 cm. These results suggest that Re is the most promising tracer for intermediate reducing conditions when oxygen is present in bottom waters but rapidly consumed from pore waters. In addition, there is minimal complication when discerning sediment Re authigenic enrichment relative to its detrital background. Rhenium detrital concentrations are extremely low relative to measured authigenic concentrations, which results in negligible error associated when calculating the authigenic fraction. Rhenium is uncomplicated by adsorption to Mn oxides and/or Fe oxyhydroxide surfaces, and Re accumulation in sediments appears to be

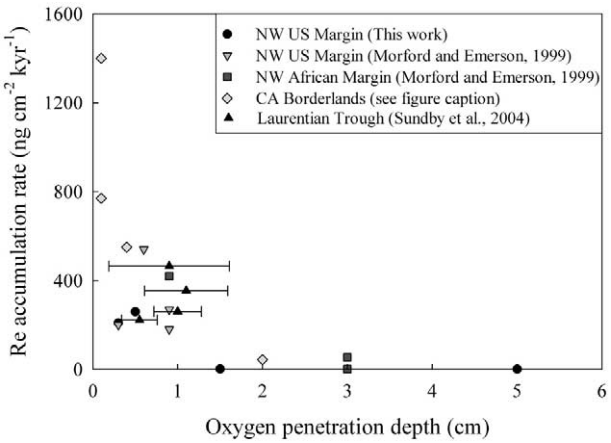

Fig. 8. Compilation of Re accumulation rate (ng cm^{-2} kyr^{-1}) plotted versus oxygen penetration depth below the sediment-water interface, as described in Table 6.

solely due to the extent of reducing conditions. Therefore, Re appears to be the best indicator for intermediate reducing conditions where oxygen penetrates less than ~1 cm below the sediment-water interface.

Coupling authigenic Re and Mo sediment concentrations should distinguish intermediate reducing conditions from oxic or anoxic conditions. The absence of Re suggests that the oxygen penetration depth is greater than 1 cm, even in the presence of sediment Mo enrichment, owing to the potential for Mo adsorption to Mn oxides. The presence of authigenic Re with negligible authigenic Mo enrichment would suggest intermediate reducing conditions, where bottom water oxygen concentrations are nonzero but oxygen goes to zero less than 1 cm below the sediment-water interface. The presence of both authigenic Re and Mo would suggest an extremely shallow oxygen penetration depth or anoxic bottom waters. Crusius et al. (1996) suggested that the ratio of Re/Mo in sediments would be useful in discerning redox conditions. Oxic conditions would have Re/Mo ratios that mimic the crustal ratio or less (depending on Mo adsorption to Mn oxides), intermediate conditions would have higher Re/Mo ratios owing to authigenic Re enrichment, and anoxic conditions would have Re/Mo ratios similar to their ratio in seawater because both Re and Mo are assumed to be quantitatively removed from seawater to sediments. However, Nameroff et al. (2002) revealed the difficulty of using Re/Mo ratios for sediments recovered from the oxygen minimum zone off Mexico, with authigenic Re and Mo accumulation suggesting anoxic conditions but Re/Mo ratios suggesting intermediate reducing conditions. Consistent with Nameroff et al. (2002), we suggest that Re/Mo ratios should be used cautiously, whereas authigenic accumulation data provides more direct evidence of the extent of reducing conditions.

5. CONCLUSION

This research has provided a valuable test of the hypothesis that trace metals respond to the extent of reducing conditions in a predictable way. The range in oxygen penetration depths along this transect fall broadly into those stations with oxygen penetration <1 cm (stations 2, 3b, and 4) and those stations with oxygen penetration >1 cm (stations 5, 6, 7, and 8). When oxygen penetrates less than 1 cm, Fe is reduced to pore waters but reoxidized near the sediment-water interface, preventing a flux of Fe^{2+} to overlying waters, whereas Mn oxides are reduced and Mn^{2+} diffuses to overlying waters. Both Re and U authigenically accumulate in sediments. Only at the most reducing location, where the oxygen penetrates 0.3 cm below the sediment-water interface, does the surface 30 cm of the sediments become reducing enough to authigenically accumulate Mo.

Stations in close proximity to the Juan de Fuca Ridge crest are enriched in Mn and Fe from hydrothermal plume processes. Both V and Mo clearly associate with Mn cycling, whereas U may be associating with either Mn oxides and/or Fe oxyhydroxides. Rhenium is uncomplicated by adsorption to sediment Mn and/or Fe, and Re accumulation in sediments appears to be solely due to the extent of reducing conditions. Therefore, coupling authigenic Re and Mo sediment concentrations should distinguish intermediate reducing conditions from either oxic or anoxic conditions. The absence of Re suggests oxic conditions, even in the presence of sediment Mo enrichment due to the potential for Mo adsorption to Mn oxides. The presence of authigenic Re with negligible authigenic Mo enrichment would suggest intermediate reducing conditions, where bottom water oxygen concentrations are nonzero but oxygen goes to zero less than 1 cm below the sediment-water interface. The presence of both authigenic Re and Mo would suggest an extremely shallow oxygen penetration depth or anoxic bottom waters.

5.1. Future Directions

Additional data continues to be necessary to constrain redox-sensitive trace metal geochemical cycling in shallow coastal areas, where bioturbation may compromise authigenic trace metal accumulation (e.g., Zheng et al., 2002), and areas with fast sedimentation rates (e.g., Sundby et al., 2004). The logical next step will be to incorporate Re into a sediment–pore water model such as Muds (Archer et al., 2002), verify the model response under present-day conditions using literature data, and then adjust the global reducing conditions to monitor the Re authigenic sediment response. Rhenium analyses in well chosen sediment cores should then provide valuable constraints on past changes in reducing conditions. The search continues for a combination of tracers that will distinguish between changes in bottom water oxygen concentration and changes in organic carbon flux to the sediment-water interface, because it is not yet possible to distinguish between an increase in carbon flux and a decrease in bottom water oxygen content from trace metal sediment profiles.

Acknowledgments—The authors thank the crew of the R/V T. G. Thompson for an extremely productive cruise. J.L.M. acknowledges the ICPMS expertise provided by Dave Schneider of the WHOI Plasma Facility. Funding for this work was provided by NSF-9911103 to S.R.E., and by the Postdoctoral Scholar Program at WHOI to J.L.M., courtesy of the Cabot Marine Environmental Science Fund and the J. Seward Johnson Fund. Extremely helpful and detailed comments from Jennifer Mckay, Philipp Böning, and an anonymous reviewer improved this manuscript. Comments from Tim Shaw also greatly improved this paper. Data in tabular form are available from J.L.M. upon request.

Associate editor: T. Shaw

REFERENCES

Adelson J. M., Helz G. R., and Miller C. V. (2001) Reconstructing the rise of recent coastal anoxia; molybdenum in Chesapeake Bay sediments. *Geochim. Cosmochim. Acta* **65** (*2*), 237–252.

Aller R. C. (1990) Bioturbation and manganese cycling in hemipelagic sediments. *Phil. Trans. R. Soc. Lond.* **A331**, 51–68.

Anbar A. D., Creaser R. A., Papanastassiou D. A., and Wasserburg G. J. (1992) Rhenium in seawater: Confirmation of generally conservative behavior. *Geochim. Cosmochim. Acta* **56,** 4099–4103.

Anderson R. F., LeHuray A. P., Fleisher M. Q., and Murray J. W. (1989) Uranium deposition in Saanich Inlet sediments, Vancouver Island. *Geochim. Cosmochim. Acta* **53,** 2205–2213.

Anderson R. F., Kumar N., Mortlock R. A., Froelich P. N., Kubik P., Dittrich-Hannen B., and Suter M. (1998) Late-Quaternary changes in productivity of the Southern Ocean. *J. Mar. Sys.* **17,** 497–514.

Archer D., Morford J., and Emerson S. (2002) A model of suboxic sedimentary diagenesis suitable for automatic tuning and gridded global domains. *Global Biogeochem. Cycles,* **16** (*1*).

Barnes C. E. and Cochran J. K. (1991) Geochemistry of uranium in Black Sea sediments. *Deep-Sea Res.* **38,** S1237–S1254.

Barnes C. E. and Cochran J. K. (1993) Uranium geochemistry in estuarine sediments: Controls on removal and release processes. *Geochim. Cosmohim. Acta* **57,** 555–569.

Bender M. L. (1971) Does upward diffusion supply the excess manganese in pelagic sediments? *J. Geophys. Res.* **76,** 4212–4215.

Breckel E. J., Emerson S., and Balistrieri L. S. (2005) Authigenesis of trace metals in energetic tropical shelf environments. *Continental Shelf Res.* **25**, 1321–1337.

Broecker W. S. and Peng T. H. (1987) The role of $CaCO_3$ compensation in the glacial to interglacial atmospheric CO_2 change. *Global Biogeochem. Cycles* **1,** 15–30.

Brumsack H. J. and Gieskes J. M. (1983) Interstitial water trace-metal chemistry of laminated sediments from the Gulf of California, Mexico. *Mar. Chem.* **14,** 89–106.

Calvert S. and Pedersen T. (1993) Geochemistry of recent oxic and anoxic marine sediments: Implications for the geological record. *Mar. Geol.* **113,** 67–88.

Calvert S. and Piper D. Z. (1984) Geochemistry of ferromanganese nodules from DOMES Site A, Northern Equatorial Pacific: Multiple diagenetic metal sources in the deep sea. *Geochim. Cosmochim. Acta* **48,** 1913–1928.

Cochran J. K., Carey A. E., Sholkovitz E. R., and Surprenant L. D. (1986) The geochemistry of uranium and thorium in coastal marine sediments and sediment pore waters. *Geochim. Cosmochim. Acta* **50,** 663–680.

Collier R. W. (1984) Particulate and dissolved vanadium in the North Pacific Ocean. *Nature* **309,** 441–444.

Collier R. W. (1985) Molybdenum in the Northeast Pacific Ocean. *Limnol. Oceanogr.* **30,** 1351–1353.

Colodner D. (1991) *The Marine Geochemistry of Rhenium, Iridium and Platinum.* Ph.D. thesis, WHOI, p. 276.

Colodner D., Sachs J., Ravizza G., Turekian K., Edmond J., and Boyle E. (1993) The geochemical cycle of rhenium: A reconnaissance. *Earth Planet. Sci. Lett*., **117,** 205–221.

Crusius J. and Thomson J. (2000) Comparative behavior of authigenic Re, U, and Mo during reoxidation and subsequent long-term burial in marine sediments. *Geochim. Cosmochim. Acta* **64** (*13*), 2233–2242.

Crusius J., Calvert S.E., Pedersen T.F., and Sage D. (1996) Rhenium and molybdenum enrichments in sediments as indicators of oxic, suboxic and anoxic conditions of deposition. *Earth Planet. Sci. Lett.* **145,** 65–79.

Davies S. H. R. and Morgan J. J. (1989) Manganese(II) oxidation kinetics on metal oxide surfaces. *J. Colloid Interface Sci.* **129,** 63–77.

Dean W., Gardner J., and Anderson R. (1994) Geochemical evidence for enhanced preservation of organic matter in the oxygen minimum zone of the continental margin of northern California during the late Pleistocene. *Paleoceangraphy* **9,** 47–61.

Dean W., Gardner J. V., and Piper D. Z. (1997) Inorganic geochemical indicators of glacial-interglacial changes in productivity and anoxia on the California continental margin. *Geochim. Cosmochim. Acta* **61,** 4507–4518.

Dean W. E., Piper D. Z., and Peterson L. C. (1999) Molybdenum accumulation in Cariaco basin sediment over the past 24 k.y.: A record of water-column anoxia and climate. *Geology* **27,** 507–510.

Devol A. H. and Hartnett H. E. (2001) Role of the oxygen-deficient zone in transfer of organic carbon to the deep ocean. *Limnol. Oceanogr.* **46** (*7*): 1684–1690.

Dymond J. (1981) Geochemistry of Nazca plate surface sediments: An evaluation of hydrothermal, biogenic, detrital, and hydrogenous sources. *Geol. Soc. Am. Mem.* **154,** 133–172.

Emerson S. (1985) Organic carbon preservation in marine sediments. In *The Carbon Cycle and Atmospheric CO_2: Natural Variations Archean to Present.* (eds. E. T. Sundquist and W. S. Broecker). American Geophysical Union.

Emerson S. R. and Huested S. S. (1991) Ocean anoxia and the concentration of molybdenum and vanadium in seawater. *Mar. Chem.* **34,** 177–196.

François R., Bacon M. P., Altabet M. A., and Labeyrie L. D. (1993) Glacial/Interglacial changes in sediment rain rate in the SW Indian sector of Subantarctic waters as recorded by ^{230}Th, ^{231}Pa, U and delta^{15}N. *Paleoceangraphy* **8,** 611–629.

François R., Altabet M. Z., Yu E-F., Sigman D. M., Bacon M. P., Frank M., Bohrmann G., Bareille G., and Labeyrie L. D. (1997) Contribution of Southern Ocean surface-water stratification to low atmospheric CO_2 concentrations during the last glacial period. *Nature* **389,** 929–935.

Froelich P. N., Klinkhammer G. P., Bender M. L., Luedtke N. A., Heath G. R., Cullen D., and Dauphin P. (1979) Early oxidation of organic matter in pelagic sediments of the eastern equatorial Atlantic: Suboxic diagenesis. *Geochim. Cosmochim. Acta* **43,** 1075–1090.

Hartnett H. E. and Devol A. H. (2003) Role of a strong oxygen-deficient zone in the preservation and degradation of organic matter: A carbon budget for the continental margins of northwest Mexico and Washington State. *Geochim. Cosmochim. Acta* **67,** 247–264.

Hartnett H. E., Keil R. G., Hedges J. I., and Devol A. H. (1998) Influence of oxygen exposure time on organic carbon preservation in continental margin sediments. *Nature* **391,** 572–574.

Heath G. R. and Dymond J. (1981) Metalliferous-sediment deposition in time and space: East Pacific Rise and Bauer Basin, northern Nazca plate. *Geol. Soc. Am. Mem.* **154,** 175–197.

Hedges J. I., Hu F. S., Devol A. H., Hartnett H. E., Tsamakis E., and Keil R. G. (1999) Sedimentary organic matter preservation: A test for selective degradation under oxic conditions. *Am. J. Sci.* **299,** 529–555.

Jeandel C., Caisso M., and Minster J. F. (1987) Vanadium behavior in the global ocean and in the Mediterranean Sea. *Mar. Chem.* **21,** 51–74.

Kienast S. S., Calvert S. E., and Pedersen T. F. (2002) Nitrogen isotope and productivity variations along the northeast Pacific margin over the last 120 kyr: Surface and subsurface paleoceanography. *Paleoceanography* **17** (*4*), 1055.

Klinkhammer G. P. and Palmer M. R. (1991) Uranium in the oceans: Where it goes and why. *Geochim. Cosmochim Acta* **55,** 1799–1806.

Klinkhammer G. P. and Hudson A. (1986) Dispersal patterns for hydrothermal plumes in the South Pacific using manganese as a tracer. *Earth Planet. Sci. Lett.* **79,** 241–249.

Knox F. and McElroy M. (1984) Changes in atmospheric CO_2: Influence of biota at high latitudes. *J. Geophys. Res.* **89,** 4629–4637.

Ku T. L., Knauss K. G., and Mathieu G. G. (1977) Uranium in the open ocean: Concentration and isotopic composition. *Deep-Sea Res*. **24,** 1005–1017.

Kyte F. T., Leinen M., Heath G. R., and Zhou L. (1993) Cenozoic sedimentation history of the central North Pacific: Inferences from the elemental geochemistry of core LL44-GPC3. *Geochim. Cosmochim. Acta* **57,** 1719–1740.

Lambourn D., Hartnett H., and Devol A. (1996) Porewater data from the Washington Shelf and Slope: Cruise WE4907B of the R/V Wecoma. In *Special Report No. 113,* School of Oceanography, Univ. Washington.

Lavelle J. W., Cowen J. P., and Massoth G. J. (1992) A model for the deposition of hydrothermal manganese near ridge crests. *J. Geophys. Res.*, **97** (C5), 7413–7427.

Lovley D. R., Phillips E. J. P., Gorby Y. A., and Landa E. R. (1991) Microbial reduction of uranium. *Nature* **350**: 413–416.

Mangini A., Jung M., and Laukenmann S. (2001) What do we learn from peaks of uranium and of manganese in deep sea sediments? *Mar. Geol.* **177,** 63–78.

Mills R., Elderfield H., and Thomson J. (1993) A dual origin for the hydrothermal component in a metalliferous sediment core from the Mid-Atlantic Ridge. *J. Geophys. Res.* **98,** 9671–9681.

Morford J. L. and Emerson S. (1999) The geochemistry of redox sensitive trace metals in sediments. *Geochim. Cosmochim. Acta* **63,** 1735–1750.

Murray R. W. and Leinen M. (1993) Chemical transport to the seafloor of the equatorial Pacific Ocean across a latitudinal transect at 135°W: Tracking sedimentary major, minor, trace and rare earth element fluxes at the Equator and the Intertropical Convergence Zone. *Geochim. Cosmochim. Acta* **57,** 4141–4163.

Myers C. R. and Nealson K. H. (1988) Microbial reduction of manganese oxides: Interactions with iron and sulfur. *Geochim. Cosmochim. Acta* **52,** 2727–2732.

Nameroff T. J., Balistrieri L. S., and Murray J. W. (2002) Suboxic trace metal geochemistry in the eastern tropical North Pacific. *Geochim. Cosmochim. Acta* **66** (*7*), 1139–1158.

Nameroff T. J., Calvert S. E., and Murray J. W. (2004) Glacial-interglacial variability in the eastern tropical North Pacific oxygen minimum zone recorded by redox-sensitive trace metals. *Paleoceanography* **19**, PA1010.

Ravizza G., Martin C. E., German C. R., and Thompson G. (1996) Os isotopes as tracers in seafloor hydrothermal systems: Metalliferous deposits from the TAG hydrothermal area, 26°N Mid-Atlantic Ridge. *Earth Planet. Sci. Lett.* **138,** 105–119.

Rodushkin I. and Ruth T. (1997) Determination of trace metals in estuarine and seawater reference materials by high resolution inductively coupled plasma mass spectrometry. *J. Anal. At. Spectrom.* **12,** 1181–1185.

Rosenthal Y., Boyle E. A., Labeyrie L., and Oppo D. (1995) Glacial enrichments of authigenic Cd and U in Subantarctic sediments: A climatic control on the elements' ocean budget? *Paleoceanography* **10,** 395–413.

Sarmiento J. L. and Orr J. C. (1991) Three-dimensional simulations of the impact of Southern Ocean nutrient depletion on atmospheric CO_2 and ocean chemistry. *Limnol. Oceanogr.* **36,** 1928–1950.

Sarmiento J. L. and Toggweiler R. (1984) A new model for the role of the oceans in determining atmospheric pCO_2. *Nature* **308,** 621–624.

Schaller T., Morford J., Emerson S., and Feely R. (2000) Oxyanions in metalliferous sediments: Tracers for paleoseawater metal concentrations? *Geochim. Cosmochim. Acta*, **63** (*13*), 2243–2254.

Shaw T. J., Gieskes J. M., and Jahnke R. A. (1990) Early diagenesis in differing depositional environments: The response of transition metals in pore water. *Geochim. Cosmochim. Acta*, **54,** 1233–1246.

Siegenthaler U. and Wenk T. (1984) Rapid atmospheric CO_2 variations and ocean circulation. *Nature* **308,** 624–625

Silverberg N., Sundby B., Mucci A., Zhong S., Arakaki T., Hall P., Landen A., and Tengberg A. (2000) Remineralization of organic carbon in eastern Canadian continental margin sediments. *Deep-Sea Res. II* **47,** 699–731.

Spears D. A. and Kanaris-Sotiriou R. (1976) Titanium in some Carboniferous sediments from Great Britain. *Geochim. Cosmochim. Acta* **40,** 345–351.

Stump C. and Emerson S. (2001) Special Report No. 117: Redox states of marine sediments from a transect along 47 N in the North Pacific Ocean: TTN 131 of the R/V T. G. Thompson.

Sundby B., Martinez P. and Gobeil C. (2004) Comparative geochemistry of cadmium, rhenium, uranium, and molybdenum in continental margin sediments. *Geochim. Cosmochim. Acta* **68,** 2485–2493.

Sung W. and Morgan J. J. (1980) Kinetics and products of ferrous iron oxygenation in aqueous systems. *Environ. Sci. Technol.* **14** (*5*), 561–568.

Tebo B. M., Nealson K. H., Emerson S., and Jacobs L. (1984) Microbial mediation of Mn(II) and Co(II) precipitation at the O_2/H_2S interfaces in two anoxic fjords. *Limnol. Oceanogr.* **29** (*6*), 1247–1258.

Thamdrup B., Fossing H., and Jorgensen B. B. (1994) Manganese, iron and sulfur cycling in a coastal marine sediment, Aarhus Bay, Denmark. *Geochim. Cosmochim. Acta*, **58,** 5115–5129.

Turekian K. K. and Wedepohl K. H. (1961) Distribution of the elements in some major units of the earth's crust. *Geol. Soc. Am. Bull.* **72,** 175–192.

Wanty R. B., Goldhaber M. B., and Northrop H. R. (1990) Geochemistry of vanadium in an epigenetic sandstone-hosted vanadium-uranium deposit, Henry basin, Utah. *Econ. Geol.* **85,** 270–284.

Wehrli B. and Stumm W. (1989) Vanadyl in natural waters: Adsorption and hydrolysis promote oxygenation. *Geochim. Cosmochim. Acta* **53,** 69–77.

Zheng Y. (1999) The marine geochemistry of germanium, molybdenum and uranium: The sinks. Ph.D. Thesis, Columbia University.

Zheng Y., Anderson R. F., van Geen A., and Fleisher M. Q. (2002) Remobilization of authigenic uranium in marine sediments by bioturbation. *Geochim. Cosmochim. Acta* **66** (*10*), 1759–1772.